

DISCOVERY OF A PULSAR WIND NEBULA CANDIDATE IN THE CYGNUS LOOP

SATORU KATSUDA¹, HIROSHI TSUNEMI², KOJI MORI³, HIROYUKI UCHIDA⁴, ROBERT PETRE⁵, SHIN'YA YAMADA¹, AND TORU TAMAGAWA¹

Draft version June 20, 2018

ABSTRACT

We report on a discovery of a diffuse nebula containing a pointlike source in the southern blowout region of the Cygnus Loop supernova remnant, based on *Suzaku* and *XMM-Newton* observations. The X-ray spectra from the nebula and the pointlike source are well represented by an absorbed power-law model with photon indices of 2.2 ± 0.1 and 1.6 ± 0.2 , respectively. The photon indices as well as the flux ratio of $F_{\text{nebula}}/F_{\text{pointlike}} \sim 4$ lead us to propose that the system is a pulsar wind nebula, although pulsations have not yet been detected. If we attribute its origin to the Cygnus Loop supernova, then the 0.5–8 keV luminosity of the nebula is computed to be $2.1 \times 10^{31} (d/540 \text{ pc})^2 \text{ ergs s}^{-1}$, where d is the distance to the Loop. This implies a spin-down loss-energy $\dot{E} \sim 2.6 \times 10^{35} (d/540 \text{ pc})^2 \text{ ergs s}^{-1}$. The location of the neutron star candidate, $\sim 2^\circ$ away from the geometric center of the Loop, implies a high transverse velocity of $\sim 1850 (\theta/2^\circ) (d/540 \text{ pc}) (t/10 \text{ kyr})^{-1} \text{ km s}^{-1}$, assuming the currently accepted age of the Cygnus Loop.

Subject headings: ISM: individual objects (Cygnus Loop) — ISM: supernova remnants — pulsars: general — stars: neutron — stars: winds, outflows — X-rays: ISM

1. INTRODUCTION

The Cygnus Loop supernova remnant (SNR), the X-ray image of which is shown in Fig.1, is one of the brightest SNRs in the X-ray sky. Because of its proximity, 540(+100, -80) pc (Blair et al. 2009), it is an extremely important object that is often called a prototypical middle-aged SNR (10 kyr: Levenson et al. 1998). The X-ray morphology is an almost perfect circular shell except for a southern blowout region. The origin of the blowout has been a matter of debate; it may be caused by either low ambient density (Aschenbach & Leahy 1999; Uchida et al. 2008) or a second SNR (Uyaniker et al. 2002; Sun et al. 2006).

Another mystery for the Cygnus Loop is the absence of a central compact remnant. It is believed that the Cygnus Loop is the result of a core-collapse SN, because the blast wave is now hitting the walls of the cavity that was most likely created by a strong stellar wind from the progenitor (e.g., Charles et al. 1985; Hester et al. 1994; Levenson et al. 1997). The comparatively small size of the cavity ($R \sim 13 \text{ pc}$ at a distance of 540 pc) led Levenson et al. (1998) to suggest that the progenitor star was of spectral type later than B0, $\sim 15 M_\odot$. This view is further supported by recent X-ray abundance measurements which have led to progenitor mass estimates of 12–15 M_\odot (e.g., Tsunemi et al. 2007; Kimura et al. 2009; Uchida et al. 2011). Such a

progenitor star should have formed a neutron star during the SN explosion. Although considerable effort has been devoted to searching for a neutron star in the Cygnus Loop over nearly three decades, none has been found yet (e.g., Miyata et al. 1998, 2001).

Here, we report on the discovery of a possible pulsar wind nebula (PWN) in the southern blowout region of the Cygnus Loop, based on X-ray observations with *Suzaku* and *XMM-Newton*. This Letter focuses on the discussion about the PWN candidate, while other results based on these data have been published elsewhere (e.g., Tsunemi et al. 2007; Uchida et al. 2011; Katsuda et al. 2011).

2. OBSERVATIONS

We have conducted over 80 pointing observations of the Cygnus Loop using the *Suzaku* X-ray Imaging Spectrometer (XIS: Koyama et al. 2007) and the *XMM-Newton* European Photon Imaging Camera (EPIC: Turner et al. 2001; Strüder et al. 2001), covering nearly the entirety of this large SNR. The fields of view (FOV) of these observations are overlaid on the *ROSAT* all-sky survey image in Fig. 1. We focus here on one XIS/EPIC observation located in the southern blowout region. The XIS and EPIC observations were performed on 2011-05-07 (Obs.ID: 506013010) and 2006-05-15 (Obs.ID: 0405490301), respectively.

For the *Suzaku* XIS data, we use cleaned event data prepared by the *Suzaku* operations team. The net exposure time is 60.3 ks for each XIS. The *XMM-Newton* data suffer severely from high background (BG) flares due to soft protons throughout the observation. Nonetheless, the EPIC image may provide us with useful information on spatial structures, thanks to much better angular resolution than the XIS. We thus use relatively clean time regions, where the count rates in the 5–12 keV are less than 5 cts s⁻¹ for MOS1/2 or 50 cts s⁻¹ for pn. The effective exposure times obtained are 7.8 ks, 8.0 ks, and

¹ RIKEN (The Institute of Physical and Chemical Research), 2-1 Hirosawa, Wako, Saitama 351-0198

² Department of Earth and Space Science, Graduate School of Science, Osaka University, 1-1 Machikaneyama, Toyonaka, Osaka, 60-0043, Japan

³ Department of Applied Physics, Faculty of Engineering, University of Miyazaki, 1-1 Gakuen Kibana-dai Nishi, Miyazaki, 889-2192, Japan

⁴ Department of Physics, Kyoto University, Kitashirakawa-oiwake-cho, Sakyo, Kyoto 606-8502, Japan

⁵ NASA Goddard Space Flight Center, Code 662, Greenbelt MD 20771

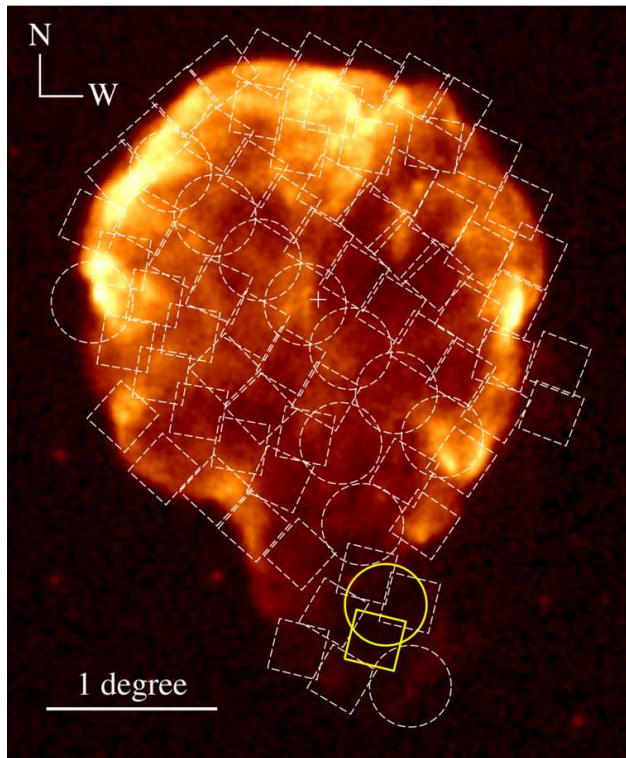


Figure 1. *ROSAT* all-sky survey image of the Cygnus Loop, scaled as the square root of the surface brightness. The energy band used is 0.2–2 keV. All of the *Suzaku* XIS and the *XMM-Newton* EPIC fields observed to date are overlaid as boxes and circles, respectively. The XIS and EPIC images of the yellow FOV is shown in Fig. 2. The geometric center of the Cygnus Loop is indicated by a cross.

6.0 ks for MOS1, MOS2, and pn, respectively. All the raw data are processed using version 11.0.0 of the XMM Science Analysis Software. Further analyses are done with `heasoft` tools of version 6.11.1 and the latest CALDB files updated on 2011-11-09.

3. ANALYSIS AND RESULTS

Through our comprehensive analyses of the X-ray data, we have discovered a hard X-ray-emitting nebula in the southern blowout region of the Cygnus Loop, i.e., the XIS/EPIC FOV illustrated in yellow in Fig. 1. Figure 2 left and center are vignetting-corrected XIS images in 0.5–1 keV and 1–10 keV, respectively, for which non X-ray BG is subtracted by using the `xisnxbgen` software (Tawa et al. 2008). While the left panel is dominated by thermal emission from the Cygnus Loop, the central panel represents mixture of cosmic X-ray BG and hard X-rays from astrophysical sources. In the hard-band image, we see a bimodal diffuse feature—our target of interest in this Letter. An *XMM-Newton* image in Fig. 2 right successfully resolves it into a northern diffuse nebula and a southern pointlike source. It should be noted that the short exposure time and the presence of soft proton events in the *XMM-Newton* image make it difficult to detect faint diffuse emission between the pointlike source and the northern nebula.

The position of the pointlike source is determined to be [RA, Dec] = [20:49:20.309, +29:01:05.57 (J2000)], by using the `emldetect` software. The statistical uncertainty

is negligible compared with the astrometric uncertainty of $2''$ (based on the *XMM-Newton* Calibration Technical Note – Guainazzi 2011). The source has been identified as 2XMM J204920.2+290106 in the *XMM-Newton* Serendipitous Source Catalog (Watson et al. 2009). No obvious optical and infrared counterpart is found in the Palomar Observatory Sky Survey and 2MASS All Sky Survey, respectively, although there is an apparent compact galaxy whose peak is $\sim 3''$ away from the X-ray pointlike source and its optical emission extends to the source position. The R-band upper limit is estimated to be $R_{\gtrsim 19}$ mag. No radio counterpart is detected in an archival VLA 1.4 GHz image. The radial profile of the pointlike source is found to be consistent with the EPIC point-spread function at the same off-axis angle. The northern nebula is positionally consistent with an infrared object 2MASX J20491447+2903237 which is identified as an extended extra galactic source (Skrutskie et al. 2006), while its extent appears to be quite small and thus there is no evidence for the physical association to the X-ray nebula.

We examine the XIS spectra of the pointlike source and the surrounding nebula. The spectral extraction regions, a $1'$ -radius circle around the pointlike source and a polygon tracing the edge of the diffuse nebula, are shown in Fig. 2 center. BG is taken from an elliptical annulus shown in Fig. 2 left and center. The BG produced in this way includes not only usual X-ray BG but also thermal emission from the Cygnus Loop itself (typically, $kT_e \sim 0.3$ keV and $n_e t \sim 10^{11}$ cm $^{-3}$ s; Uchida et al. 2008).

The XIS0+3 spectra together with the area-normalized local-BG spectra are shown in the upper panels of Fig. 3, and the local-BG subtracted spectra are plotted in the lower panels. The photon numbers after BG subtraction are 753 and 4534 for the pointlike source and the nebula, respectively. Since emission below 1.5 keV is dominated by Cygnus Loop’s thermal emission, it is in principle difficult to subtract the local BG properly in the soft X-ray band. We thus use the 1.5–10 keV band for spectral analysis. In this case, the intervening column density cannot be constrained, so we tentatively fix the value of N_H to 4×10^{20} cm $^{-2}$ which is typical for the Cygnus Loop (e.g., Inoue et al. 1980). Before fitting, each spectrum is grouped into bins with at least ~ 50 counts in prior to background subtraction, which allows us to perform a χ^2 test. In the calculation of χ^2 values, we use the standard weighting method, i.e., the square root of detected counts.

We find that either a power-law model or an optically thin thermal emission model (`appec`: Smith et al. 2001) can adequately describe the data. The thermal emission model, however, requires a high electron temperature of 2–4 keV, and very low abundances of $\lesssim 0.8$ times the solar value. Such a high temperature has never been reported from the Cygnus Loop (e.g., Tsunemi et al. 2007), and the low abundances are unusual in astrophysical sources. We thus reject the thermal model from an astrophysical point of view. Also, a blackbody model is safely rejected from a statistical point of view. Adding a blackbody or thermal emission component to the power-law component does not improve the fits, either. In this way, we conclude that the power-law is the most reasonable model to describe the data. The best-fit parameters from

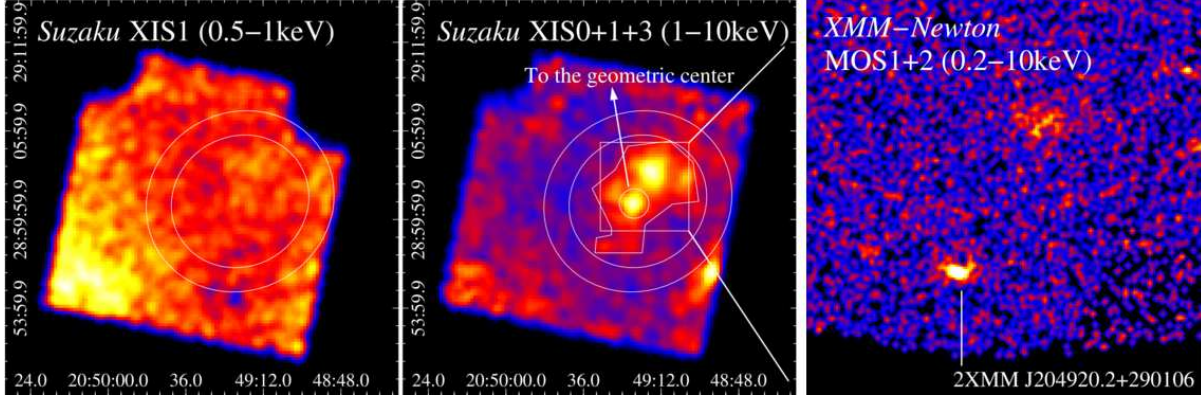


Figure 2. Left: Soft-band (0.5–1 keV) XIS1 image of the yellow box in Fig. 1. The image is scaled as a square root of the surface brightness and corrected for vignetting effects after subtraction of non X-ray BG. A white elliptical annulus shows where we extract a local BG. Center: Same as left but in the hard band. The data taken by XIS0, XIS1, and XIS3 are summed to improve photon statistics. The spectral extraction regions are shown as a white circle (for the pointlike source) and a polygon (for the nebula). Right: Closeup image of the white box ($6'$ square) in Fig. 2 center taken by the *XMM-Newton* MOS1+2. BG is not subtracted and vignetting effects are not corrected.

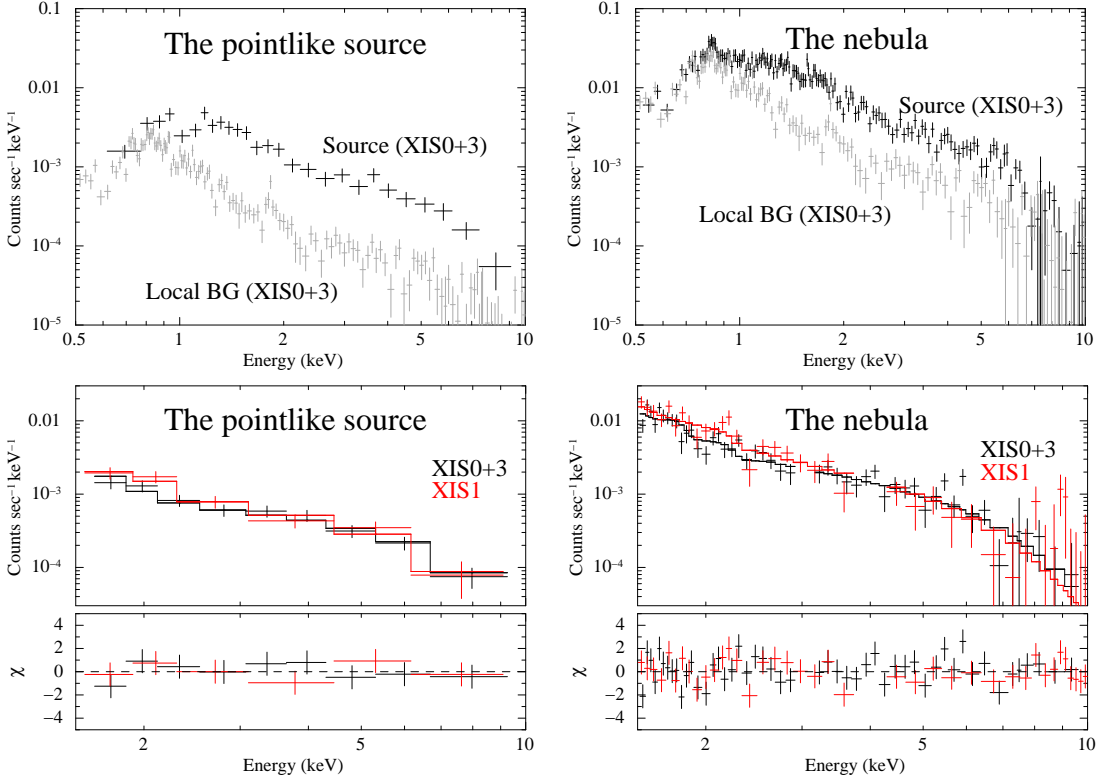


Figure 3. Left upper: *Suzaku* XIS (0+3) spectrum for the pointlike source (black) and for the area-normalized BG spectrum (gray). Right upper: Same as left but for the diffuse nebula. Left lower: Local-BG subtracted XIS spectra for the pointlike source along with the best-fit power-law model. Black and red correspond to the FI (XIS0+3) and the BI (XIS1), respectively. Lower panel shows residuals. Right lower: Same as left but for the diffuse nebula.

the power-law model are summarized in Table 1. We note that consistent results are obtained if we let the soft X-ray band (i.e., 0.5–1.5 keV) remain and fit the spectra by a power-law plus local-BG model whose normalization is allowed to vary freely. Also, no significant spatial variation of the photon index in the synchrotron nebula has been detected owing to insufficient photon statistics.

To search for long-term spectral variability of the pointlike source, we also fit the EPIC spectra. While the

Table 1
Power-law spectral-fit parameters

Region	Γ	Flux ^a	$\chi^2/\text{d.o.f.}$
The pointlike source	1.6 ± 0.2	2.0 ± 0.5	6.6/12
The nebula	2.2 ± 0.1	$5.5^{+0.7}_{-0.6}$	96.1/86

Note. — Errors quoted are at 90% confidence level.
^a Unabsorbed 0.5–8 keV flux in units of $10^{-13} \text{ ergs s}^{-1} \text{ cm}^{-2}$.

data are affected by soft protons, flux estimates would be relatively robust if we subtract a local BG. We find that the fluxes (and photon indices) inferred from the MOS and pn spectra are marginally consistent with those inferred using the XIS. In addition, a Fourier search does not give significant pulsations. This might be due to poor photon statistics as well as insufficient time resolution (0.073 s, 2.6 s, and 8 s for pn, MOS, and XIS, respectively).

4. DISCUSSION

We have presented the discovery of a diffuse nebula in the Cygnus Loop containing a pointlike source. The spectra of both are well represented by a power-law model, reminding us of a PWN. A PWN origin is further supported by the following observational features. Kargaltsev & Pavlov (2008) reported a strong correlation between PWN luminosities and the nonthermal luminosities of pulsars, namely $L_{\text{PWN}(0.5-8\text{ keV})}/L_{\text{PSR}(0.5-8\text{ keV})}$ is nearly constant at 4. Our measured $L_{\text{nebula}(0.5-8\text{ keV})}/L_{\text{pointlike}(0.5-8\text{ keV})}$ of ~ 3.8 is in good agreement with this correlation. Above, we assume that the nebula extends over the pulsar candidate with its mean surface brightness, resulting in $F_{\text{nebula}(0.5-8\text{ keV})} \sim 5.7 \times 10^{-13} \text{ ergs cm}^{-2} \text{ s}^{-1}$ and $F_{\text{pointlike}(0.5-8\text{ keV})} \sim 1.5 \times 10^{-13} \text{ ergs cm}^{-2} \text{ s}^{-1}$. Furthermore, the measured photon indices are consistent with those of PWNe, and the nebula's photon index is too hard to be interpreted as shell emission from relativistic particles accelerated at an SNR shock (generally, $\Gamma \sim 2.5 - 3$). It should be also noted that the spectrum of the nebula is softer than the pointlike source, typical of PWNe. From a morphological point of view, the brightest part of the nebula is offset from the pointlike source. This is unusual for PWNe, but complicated structures are often found in PWNe (e.g., Kargaltsev & Pavlov 2008); hence the morphology cannot be a strong reason to eliminate the PWN hypothesis. Also, the pointlike source is not likely to be a background active galactic nucleus or a foreground normal star, since it has no obvious radio or optical counterpart and its X-ray spectrum is too hard for a normal star. While low mass X-ray binaries (LMXBs) have high X-ray to optical luminosity ratios, this possibility is ruled out from the low X-ray flux of the pointlike source, $F_{2-10\text{ keV}} \sim 1.3 \times 10^{-13} \text{ ergs cm}^{-2} \text{ s}^{-1}$ based on the XIS; a normal LMXB luminosity of $\sim 10^{36} \text{ ergs s}^{-1}$ requires a distance of 250 kpc which is far outside the Galaxy. On the other hand, these properties are consistent with the expectations for an isolated neutron star, even though the conclusive evidence of a pulse period is lacking. Nevertheless, we propose that this system is a PWN.

We note, however, another possibility: that the system consists of a galaxy cluster and an unknown pointlike source which might not be related to the cluster. A brief justification can be made by comparing the nebula's properties with those of galaxy clusters. A L_X -temperature correlation of galaxy clusters (e.g., Fukazawa et al. 2004) would result in nebula's luminosity, $L_{2-10\text{ keV}} = 2.0 \times 10^{44} (kT/3\text{ keV})^{2.79} \text{ ergs s}^{-1}$. Combining the luminosity with nebula's flux, $F_{2-10\text{ keV}} = 2.7 \times 10^{-13} \text{ ergs s}^{-1}$, we obtain a distance of $\sim 2.5 \text{ Gpc}$. The apparent radius of $3'$ can be then translated to a

real radius of $\sim 2(d/2.5\text{ Gpc}) \text{ Mpc}$, which is typical for galaxy clusters with kT of 3 keV (Fukazawa et al. 2004). Therefore, the X-ray luminosity, temperature, and size are all in agreement with those of galaxy clusters. In addition, based on the *ROSAT* PSPC survey of galaxy clusters (Burenin et al. 2007), a surface density of clusters is $\sim 0.3 \text{ deg}^{-2}$ at $\sim 2.8 \times 10^{-13} \text{ ergs cm}^{-2} \text{ s}^{-1}$ which is the nebula's brightness in 0.5-2 keV. Given the Cygnus Loop's large dimension of $\sim 10 \text{ degree}^2$, we expect ~ 3 clusters inside the Loop. Thus, a chance probability to detect a galaxy cluster in the Loop is fairly large.

While other possibilities have not been excluded, this system is most likely a PWN based on its observed properties. We thus further discuss the PWN scenario. Whether it is physically associated with the Cygnus Loop is an important point. Evidence favoring a common origin is the fact that, even though the Cygnus Loop should have originated from a core-collapse SN, our survey of the *Suzaku* and *XMM-Newton* data has not detected any PWN or neutron star except for the PWN candidate disclosed here. If the objects are associated, then the distance to the PWN should be the same as the Cygnus Loop, i.e., $d \sim 540 \text{ pc}$ (Blair et al. 2005). If this is the case, the 0.5-8 keV luminosities of the pulsar candidate and the nebula are computed to be $5 \times 10^{30} (d/540\text{ pc})^2 \text{ ergs s}^{-1}$ and $2.1 \times 10^{31} (d/540\text{ pc})^2 \text{ ergs s}^{-1}$, respectively. This would be one of the lowest luminosities measured from the ~ 50 known X-ray PWNe (Kargaltsev & Pavlov 2008). The physical size of the nebula would be $\sim 0.5 (\theta_r/3')(d/540\text{ pc}) \text{ pc}$, where θ_r is the angular radius of the nebula. This size is an order of magnitude smaller than expected based on the PWN size-age relation reported by Bamba et al. (2010). This discrepancy is mitigated if the PWN is farther away than the Cygnus Loop. Therefore, the PWN candidate is either a distant, ordinary PWN unrelated to the Cygnus Loop or a nearby, peculiar PWN. This point should be revisited by future detailed X-ray spectroscopy that will allow for an N_{H} measurement.

We next estimate some important parameters, as is usually performed for putative PWNe (e.g., Hughes et al. 2001; Olbert et al. 2003; Gaensler et al. 2003). A well-known relation between PWN luminosity and spin-down loss power, $\eta \equiv L_X/\dot{E} \sim 8 \times 10^{-5}$ (most recently, Vink et al. 2011), indicates that $\dot{E} \sim 2.6 \times 10^{35} (d/540\text{ pc})^2 \text{ ergs s}^{-1}$. The estimated \dot{E} allows us to deduce a pulsar period of $P \sim 0.48 [2/(n-1)]^{0.5} (\dot{E}/2.6 \times 10^{35} \text{ ergs s}^{-1})^{-0.5} (t/10\text{ kyr})^{-0.5} \text{ s}$, assuming a standard moment of inertia ($I = 10^{45} \text{ g cm}^2$, i.e., a standard neutron star radius of 10 km and a mass of $1.4 M_{\odot}$), a braking index of 3, and a negligible initial period. Also, the period derivative can be estimated to be $\dot{P} = P/[(n-1)t] \sim 7.7 \times 10^{-13} (\dot{E}/2.6 \times 10^{35} \text{ ergs s}^{-1})^{-0.5} (t/10\text{ kyr})^{-1.5} \text{ s s}^{-1}$, leading to a surface magnetic field estimate of $B \sim 1.9 \times 10^{13} (\dot{E}/3.4 \times 10^{35} \text{ ergs s}^{-1})^{-0.5} (t/10\text{ kyr})^{-1} \text{ G}$. Comparing these parameters with those of the other X-ray-emitting PWNe (Kargaltsev & Pavlov 2008), we find that \dot{E} is somewhat smaller than others derived at the age of 10 kyr and that the P and B values are among the largest of all the listed PWNe. Alternatively, noting that there is a correlation between \dot{E} and τ , $\dot{E} = 41.1 - 1.08 \log \tau$

for $\tau < 10^4$ kyr, we can infer τ for the estimated \dot{E} of $2.6 \times 10^{35} (d/540 \text{ pc})^2 \text{ ergs s}^{-1}$ to be ~ 180 kyr. This would lead to $P \sim 112$ ms and $B \sim 10^{12}$ G, which are common for X-ray PWNe (Kargaltsev & Pavlov 2008). We also point out that the estimated \dot{E} implies a gamma-ray luminosity for a possible pulsar of $1.6 \times 10^{34} (\dot{E}/2.6 \times 10^{35} \text{ ergs s}^{-1})^{-0.5} \text{ ergs s}^{-1}$ in 0.1–100 GeV (Abdo et al. 2010). This should be easily detected with the *Fermi* LAT, which is not the case (Katagiri et al. 2011).

It is interesting to note that the neutron star candidate is located far from Cygnus Loop's geometric center defined by *Einstein* (Ku et al. 1984), as can be seen in Fig. 1. If we assume that the pointlike source started moving from the geometric center 10 kyr ago, its transverse velocity is $\sim 1850 (\theta/2^\circ)(d/540 \text{ pc})(t/10 \text{ kyr})^{-1} \text{ km s}^{-1}$, and its proper motion $\sim 0''.72 (\theta/2^\circ)(t/10 \text{ kyr})^{-1} \text{ yr}^{-1}$, where θ is the angular distance between the neutron star candidate and the geometric center and t is the best-estimated age of the Cygnus Loop. Such a high velocity is one of the fastest of known neutron stars (e.g., Kaspi et al. 2006). However, we should keep in mind that the velocity estimate is quite uncertain. The explosion location is quite uncertain (and thus θ), because the SN went off in a cavity. In fact, it has been proposed that the SN occurred in the southern blowout region (Tenorio-Tagle et al. 1985). The age is also a matter of debate; it might not be accurate to 50%.

We have checked that the existing data including *Einstein*, *ROSAT*, and *ASCA* do not allow us to measure the proper motion of the source; the source is not detected, possibly due to insufficient exposure times as well as low detection efficiency in the hard X-ray band. It is also difficult to measure proper motions using the XIS data, given the large position uncertainty of $\sim 1'$ due to thermal fluctuation (Uchiyama et al. 2008). Thus, high-resolution images with *Chandra* or *XMM-Newton* will be required. Confirmation of a large proper motion towards the south would be direct evidence that the pointlike source is indeed the neutron star remnant of the Cygnus Loop. In this case, we expect a cometary bowshock structure around the neutron star (cf. Gaensler et al. 2004) due to the high Mach number of ~ 6 , given a reasonable sound speed of $c_s = \sqrt{(\gamma kT)/(\mu m_p)} \sim 300 \text{ km s}^{-1}$, where γ is a specific heat ratio (5/3), kT is the plasma temperature (0.3 keV), and μ is the mean molecular mass (~ 0.6 for solar abundance plasmas), and m_p is the proton mass. Note that such a bow shock would be directed away from the geometric center of the Loop and thus not necessarily related to the northern nebula. A much higher Mach number would be expected if the system is already outside the hot plasma and is now proceeding into cold interstellar medium. On the other hand, if the proper motion turns out to be small, the location of the PWN candidate near the center of the blowout appears to support the suggestion that the southern blowout is a separate SNR (Uyaniker et al. 2002).

5. CONCLUSION

Using *Suzaku* and *XMM-Newton*, we discovered a hard X-ray-emitting diffuse nebula containing a pointlike source in the southern blowout region of the Cygnus Loop. Their properties suggest that it is most likely a

PWN. The physical relation to the Cygnus Loop is still uncertain at this point. Future observations are essential in order to confirm that the object is a PWN as well as to clarify whether it is associated with the Cygnus Loop.

We would like to thank Drs. Teruaki Enoto and Takao Kitaguchi for fruitful discussions. S.K. and S.Y. are supported by the Special Postdoctoral Researchers Program in RIKEN. This work is partly supported by a Grant-in-Aid for Scientific Research by the Ministry of Education, Culture, Sports, Science and Technology (23000004).

REFERENCES

- Abdo, A. A., et al. 2010, *ApJS*, 187, 460
 Aschenbach, B., & Leahy, D. A. 1999, *A&A*, 341, 602
 Burenin, R. A., Vikhlinin, A., Hornstrup, A., Ebeling, H., Quintana, H., Mescheryakov, A. 2007, *ApJS*, 172, 561
 Bamba, A., Anada, T., Dotani, T., Mori, K., Yamazaki, R., Ebisawa, K., & Vink, J. 2010, *ApJL*, 719, 116
 Blair W. P., Sankrit, R., & Raymond, J. C. 2005, *AJ*, 129, 2268
 Blair, W. P., Sankrit, R., Torres, S. I., Chayer, P., & Danforth, C. W. 2009, *ApJ*, 692, 335
 Charles, P. A., Kahn, S. M., & McKee, C. F. 1985, *ApJ*, 295, 456
 Frail, D. A., Scharringhausen, B. R. 1997, *ApJ*, 480, 364
 Fukazawa, Y., Makishima, K., & Ohashi, T. 2004, *PASJ*, 56, 965
 Gaensler, B. M., van der Swaluw, E., Camilo, F., Kaspi, V. M., Baganoff, F. K., Yusef-Zadeh, F., & Manchester, R. N. 2004, *ApJ*, 616, 383
 Gaensler, B. M., Hendrick, S. P., Reynolds, S. P., & Borkowski, K. J. 2003, *ApJ*, 594, L111
 Gotthelf, E. V. 2003, *ApJ*, 591, 361
 Guainazzi, M. 2011, XMM-EPIC Status of Calibration and Data Analysis (XMMSOC-CAL-TN-0018)
 Hester, J. J., Raymond, J. C., & Blair, W. P. 1994, *ApJ*, 420, 721
 Hughes, J. P., Slane, P. O., Burrows, D. N., Garmire, G., Nousek, J. A., Olbert, C. M., & Keohane, J. W. 2001, *ApJ*, 559, L153
 Inoue, H., Koyama, K., Matsuoka, M., Ohashi, T., Tanaka, Y., & Tsunemi, H. 1980, *ApJ*, 238, 886
 Kargaltsev, O., & Pavlov, G. G. 2008, *AIPC*, 983, 171
 Kaspi, V. M., Roberts, M. S. E., & Harding, A. K. 2006, *csxs.book* 279 (arXiv:astro-ph/0402136)
 Katagiri, H., et al. 2011, *ApJ*, 741, 44
 Katsuda, S., et al. 2011, *ApJ*, 730, 24
 Kimura, M., Tsunemi, H., Katsuda, S., & Uchida, H. 2009, *PASJ*, 61, S137
 Koyama, K., et al. 2007, *PASJ*, 59, S221
 Ku, W. H.-M., Kahn, S. M., Pisarski, R., & Long, K. S. 1984, *ApJ*, 278, 615
 Levenson, N. A. et al. 1997, *ApJ*, 484, 304
 Levenson, N. A., Graham, J. R., Keller, L. D., & Richter, M. J. 1998, *ApJS*, 118, 541
 Miyata, E., Tsunemi, H., Torii, K., Hashimoto, K., Tsuru, T., Koyama, K., Ayani, K., Ohta, K., & Yoshida, M. 1998, *PASJ*, 50, 475
 Miyata, E., Ohta, K., Torii, K., Takeshima, T., Tsunemi, H., Hasegawa, T., & Hashimoto, Y. 2001, *ApJ*, 550, 1023
 Olbert, C. M., Keohane, J. W., Arnaud, K. A., Dyer, K. K., Reynolds, S. P., & Safi-Harb, S. 2003, *ApJ*, 592, L45
 Smith, R. K., Brickhouse, N. S., Liedahl, D. A., & Raymond, J. C. 2001, *ApJ*, 556, L91
 Skrutskie, M. F., et al. 2006, *ApJ*, 131, 1163
 Strüder, L., et al. 2001, *A&A*, 365, L18
 Sun, X. H., Reich, W., Han, J. L., Reich, P., & Wielebinski, R. 2006, *A&A*, 447, 937
 Tawa, N., et al. 2008, *PASJ*, 60, S11
 Tenorio-Tagle, G., Rozyczka, M., & Yorke, H. W. 1985, *A&A*, 148, 52
 Tsunemi, H., Katsuda, S., Nemes, N., & Miller, E. D. 2007, *ApJ*, 671, 1717
 Turner, M. J. L., et al. 2001, *A&A*, 365, L27
 Uchida, H., Tsunemi, H., Katsuda, S., & Kimura, M. 2008, *ApJ*, 688, 1102

- Uchida, H., Tsunemi, H., Tominaga, N., Katsuda, S., Kimura, M.,
Kosugi, H., Takahashi, H., & Takakura, S. 2011, PASJ, 63, 199
- Uchiyama, Y., et al. 2008, PASJ, 60, S35
- Uyaniker, B., Reich, W., Yar, A., Kothes, R., & Füst, E. 2002,
A&A, 389, L61
- Vink, J., Bamba, A., & Yamazaki, R. 2011, 727, 131
- Watson, M., et al. 2009, A&A, 493, 339